

# The Verification Significant Wave Height Technique in Indonesian Waters and Analysis of Low Air Pressure

Eko Supriyadi<sup>a,b,\*</sup>, Sri Puji Rahayu<sup>c</sup>

<sup>a</sup>Department of Geophysics and Meteorology, IPB University, Darmaga, Bogor, 16680, Indonesia

<sup>b</sup>Center for Marine Meteorology, Meteorology Climatology and Geophysical Agency (BMKG), Kemayoran, Jakarta, 10720, Indonesia

<sup>c</sup>Senior Engineering at Center for Research and Development, Meteorology Climatology and Geophysical Agency (BMKG), Kemayoran, Jakarta, 10720, Indonesia

Corresponding author: \*eko.supriyadi@bmgk.go.id

**Abstract**— A limited number of marine meteorological instruments for making observations in Indonesian waters are problems in verifying the BMKG-OFS model. The satellite altimetry was selected as a verification tool due to its wide measurement range. The verification was carried out by adjusting the coordinates, time, and grid of SWH obtained and orbit of the satellite path from the satellite altimetry to the model and overlaying the models' results as a pattern analysis in July 2018 – June 2019. The next step was a statistical analysis to determine the performance of the model. The analysis obtained 43% maximum SWH formed due to the low-pressure centers in the Pacific Ocean. The remaining spreads across the South China Sea, Indian Ocean, Andaman Sea and the Gulf of Australia. This study revealed that the SWH values from satellites were higher than the model. On every three hourly and monthly bases, the SWH of the bias, RMSE, and correlation coefficient were equivalent. The lowest bias of 0.26 occurred at 9.00 UTC, the lowest RMSE of 0.48 occurred at 21:00 UTC, and the maximum correlation coefficient of 0.82 occurred at 18:00 UTC. Whereas on a monthly scale, the lowest bias and RMSE, and the maximum correlation coefficient occurred in November. Based on these results, the BMKG-OFS model can be used to predict SWH in Indonesian waters. Besides, this verification technique can be an alternative as a new tool to verify maritime weather in the operational of BMKG.

**Keywords**— Altimetry; Indonesia waters; low pressure; OFS model; SWH; verification.

Manuscript received 26 Jun. 2020; revised 20 Jan. 2021; accepted 31 Jan. 2021. Date of publication 30 Jun. 2021.  
IJASEIT is licensed under a Creative Commons Attribution-Share Alike 4.0 International License.



## I. INTRODUCTION

Indonesia has a two-thirds area of water and the second-longest coastline globally, creating the potential resource and risk that change over time [1], [2]. One of the potentials and risks is the Significant Wave Height (SWH). SWH is the mean wave height of one-third of the measured waves [3]. A good SWH observation is carried out on a ship in the middle of the sea through the Voluntary Observing Ships (VOS) program, which has the longest continuity from 1888-present [4]. However, this method is considered inefficient to be done daily, covering a wide range of oceans. Thus, other approaches such as modeling and remote sensing were carried out. Remote sensing in this study refers to the utilization of Satellite altimetry.

Satellite altimetry has been used since the 2008s; the latest use until now is Jason 3, after the termination of Jason-2 on 17 January 2016 [5], [6]. Although there are other satellites

such as SARAL and CryoSat-2, Jason 2 is relatively constant in measuring and providing data. Satellite altimetry works by selecting the area underneath based on cycles and passes, producing location data (longitude and latitude) that is not constant over time [7]. Therefore, further processing is required for analysis. It is a challenge to develop a technique for the data generated to be used further.

Another SWH observation method is modeling. A model tends to use a mathematical approach and assumptions in the predictions so that the results tend to be different from reality [8]. In regard to the use of the model, the Marine Meteorological Center (MMC) at the Meteorological, Climatological and Geophysical Agency (BMKG) currently has a marine weather model (OFS-models) implemented since the end of 2016, including the SWH predictions. This model refers to the Wave Watch III (WW3) model, which is a third-generation wave model developed by the National Centers for Environmental Prediction (NCEP), the part of the National Oceanic and Atmospheric Administration (NOAA).

Very few satellite altimetry is currently used as verification tools for the model [9]–[12].

Therefore, a technique is needed in verifying waves between model-derived data and satellite altimetry observations. Research conducted by Appendini *et. al.* [14] presents a distinctive wave model verification concept compared to the previous techniques. In the study, the model-derived data is compared to the altimetry data that corresponds to the satellite's orbital position. However, its application requires a long way in creating a physical parameters time group as observed from the coordinates of the grid used. It also requires more than one software.

Reflecting upon the two methods above, this study verifies the OFS-SWH model towards the satellite altimetry measurements. By far, there has never been a detailed verification of the OFS model for the whole year. In addition, after the verification data is collected, the time the model provides the best results is not provided. Therefore, this paper presents a recap of the OFS-SWH model's verification towards the satellite altimetry measurements for one full year (i.e., July 2018 – June 2019) and shows the model's time shows its best performance from the statistical analysis.

## II. MATERIALS AND METHOD

The verification was carried out July 2018 – June 2019 in the coordinates  $90^{\circ}$  –  $145^{\circ}$  east latitude,  $15^{\circ}$  north –  $15^{\circ}$  south longitude. The data used are altimetry data retrieved from <ftp://eftp.ifremer.fr/>, and OFS-model retrieved from <http://peta-maritim.bmkg.go.id/render/>. Both require login accessed. The verification is limited to the SWH parameter. The verification method was conducted by adjusting the coordinates and time of the OFS model and satellite data. In general, the adjustment was made by making intervals of coordinates from satellite data to represent the model coordinates. For satellite, time synchronization was done by adjusting to the modeling time format with intervals of 3 hours. The next step was to overlay the OFS model results to find out the similarity in value. Besides, the SWH plotting time series were performed for each satellite path. It is worth noting the altimetry data used was the along-track mono-mission technique, the combination of Jason 2, Cryosat, and Saral. This technique records all SWH along the satellite path.

Since the altimetry produced non-constant location data every time result from the cycle and pass trajectory, a grid structure is needed. In a grid structure, each coordinate range is given a grid index. This grid-indexing method provides two advantages: faster processing and a better contour for further analysis. In this study, the grid size used was  $0.5^{\circ}$ . After determining the grid values, the coordinates and time adjustment were performed in the following steps:

### A. Satellite Coordinate Settings

At this stage, the longitude coordinate system setting uses the equation as follows:

$$\text{lon}_{(n+1)} = \text{lon}_{\min} + \sum_{n=0}^a 0.5n \quad (1)$$

with

$$a = \frac{\text{lon}_{\max} - \text{lon}_{\min}}{0.5} \quad (2)$$

$n$  ranges from 0 to  $a-1$ . The values of the satellite altimeter coordinate are transformed into a range of values with the equation:

$$\text{lon}_{(n+1)} \leq x < \text{lon}_{(n+2)} = n + 1 \quad (3)$$

This method enables a faster and more efficient calculation, especially over large areas. The same method is performed for the latitude.

### B. Satellite Data Timing Setting

As previously described, the BMKG-OFS time input is in the interval of 3 hours for all model parameters. Thus, the time adjustment was conducted by setting all satellite measurements at 1.5 hours before and after the main time. This is done to ensure that data from the satellite is following the main time section. After the grouping, each main time was given a sequence number from number 1 to finish, adjusting the full version's main time. This is crucial since the satellite altimetry only records the water's physical parameters without an observation of the land.

### C. Grid Settings on the Model

The grid settings in the altimetry data is intended to group the coordinates and data into a particular grid value. The use of the grid in the model adjusts to the grid generated from the altimetry data processing. The model's grid settings are intended to produce smoother images and plot data to be overlapped with the satellite trajectories. The initial grid of BMKG-OFS was  $0.0625^{\circ}$ . It was then interpolated to a new grid of  $0.01^{\circ}$ . The selection of the  $0.01^{\circ}$  value is based on the ability of the computer available for a quick calculation. It is possible to reduce the value of the grid model in order to obtain accurate data ranges and smoother map contours. The interpolation equation is as:

$$f_1(x) = f(x_0) + \frac{f(x_1) - f(x_0)}{x_1 - x_0}(x - x_0) \quad (4)$$

where:

$x$  and  $f_1(x)$  is the point to be sought through interpolation.

$x_0$  and  $f(x_0)$  is the first known data point.

$x_1$  and  $f(x_1)$  is the second known data point.

### D. Model Data Coordinate Setting

The main principle in this setting is similar to point II-A. However, the calculated number of coordinates adjusts to the time length of the model since the main time is multiplied by 3.

### E. Model Data Timing Setting

In the BMKG-OFS system, the SWH data used was updated every 00 UTC and 12 UTC. The distinction between the two lies in the WW3 input with a time difference of 12 hours. In this study, the only data taken is at 00:00 UTC, which provides the forecast for the next 7 days. Thus, eight data observations were sufficient. Each observation was 3 hours, representing one day of observation. The remaining were ignored, for they are the predictions for the next 6 days. The time setting was not performed since the OFS system's data will be compared to the 3 hours intervals.

## F. Statistical Analysis

The previous steps resulted in two main SWH data: the SWH data from the altimetry observation and that from the OFS system, which is ready to be overlapped in one map. In the overlapping process, a maximum of eight types of verification contour maps will be produced. The types represent the 3 hour-per-day observation. The results depend on observations of satellite altimetry over Indonesian waters. The next step is a validation performed by statistical analysis through the following equations:

$$\text{bias} = \frac{1}{n} \sum_{i=1}^n (m_i - o_i) \quad (5)$$

$$\text{RMSE} = \sqrt{\frac{\sum_{i=1}^n (m_i - o_i)^2}{n}} \quad (6)$$

$$\text{CC} = \frac{\sum_{i=1}^n (o_i - \bar{o})(m_i - \bar{m})}{\sqrt{\sum_{i=1}^n (o_i - \bar{o})^2 \sum_{i=1}^n (m_i - \bar{m})^2}} \quad (7)$$

where:

- RMSE = Root Mean Square.
- CC = Coefficient Correlation.
- $m_i$  = BMKG-OFS model output.
- $o_i$  = altimetry measurements.
- $\bar{m}$  = the mean of BMKG-OFS model output.
- $\bar{o}$  = the mean of altimetry measurements.

## III. RESULTS AND DISCUSSION

### A. Altimetry and OFS Model

Fig. 1 depicts an example of overlapping satellite altimeter SWH with the OFS system in the east and west monsoon. The model-derived data and satellite altimetry data were made similar to the matrix resolution for the overlapping process. The model resolution of 881x481 was adjusted to 3001x5501. The resolution adjustment did not affect the contours produced as the interpolation used was the linear interpolation. The linear interpolation refers to the changes in resolution at one point to be adjusted to the points around it linearly up to the last point. The Indonesian waters in two monsoons were generally calm, with an average wave height below 1 meter. Meanwhile, the wave outside Indonesian waters was higher. The Pacific Ocean is relatively calmer in the east monsoon (Fig. 1a) than the west monsoon (Fig. 1b). Further studies are needed to see the effect of monsoons on the SWH values in Indonesian waters.

While the lower panel of Fig. 1a and 1b (graph) presents a time series plot of the model output with satellite observations. The model-derived output was higher than that measured by the altimetry satellite. The high values of the WW3 model are a separate note due to the uncertain factors that influence it. Observed in detail, the plot from satellite observations has highly fluctuated since the observations were made every time; times, the value tended to fluctuate extremely. This is due to the change in the satellite altimetry trajectory measurement (maintaining zero compared to *nan*). Figures 1a and 1b show 2 and 3 satellite trajectories, respectively. On 15 July 2018, the fluctuations occurred on the x-axis at the values of 800 and on 15 January 2019, the fluctuations occurred on the x-axis at values of 180 and 900.

Fig.1a and 1b are just two examples of the 1358 satellite trajectories in July 2018 – June 2019.

Appendini *et. al.* [13] compared the mean of SWH, and standard deviation of altimetry data using the model obtained the same location. However, when the pressure center was low, the maximum SWH value obtained from the altimetry and model showed different locations. In the next subsection, the extreme value distribution of SWH due to the low-pressure center can be obtained from the OFS model and can be detected by the same altimetry trajectory. In addition, the total altimetry trajectory that passes Indonesian waters in July 2018 – June 2019 is presented in Figure 2.

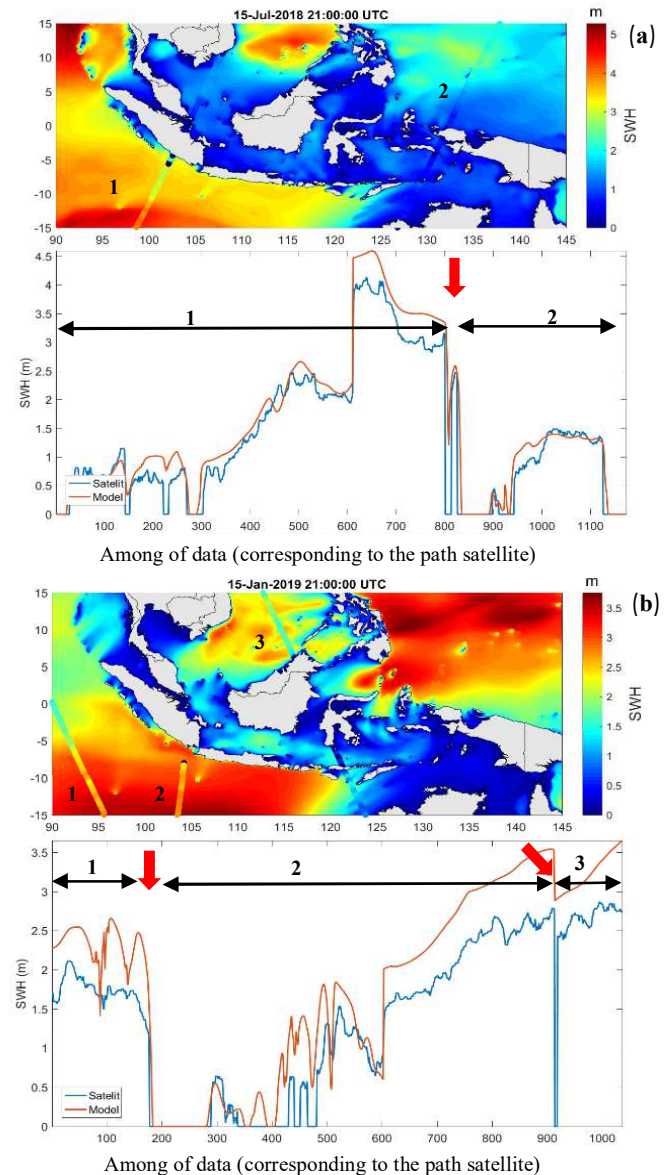


Fig. 1 (a) Result of the overlay SWH of the model (contour on the map) with altimetry satellite (straight colored line) on the top panel and time series plot of the comparison model with satellite in the west monsoon on the bottom panel. (b) Same as part a, but in the east monsoon. The red arrow indicates change in satellite trajectory (marked by numbers)

It delineates that the total trajectories fluctuate each month, with the most trajectories of 179 in December and the least of 73 in June. Normally altimetry data will be filled every 3 hours in one day. This means that there will be a minimum of

240 trajectories per month. However, this rarely happens since satellite altimetry never crosses at consecutive observations. The calculation results obtained that higher percentage SWH observation satellites are higher when compared to the model results for a weak category ( $\leq 2$  m). However, for the strong category ( $>2$  m) high percentage SWH observation of satellite is lower when compared to the model. This is the absence of territorial divisions based on the bathymetry range because, as is known generally Indonesian waters are shallow, and beyond, it is generally deep (see Fig. 1).

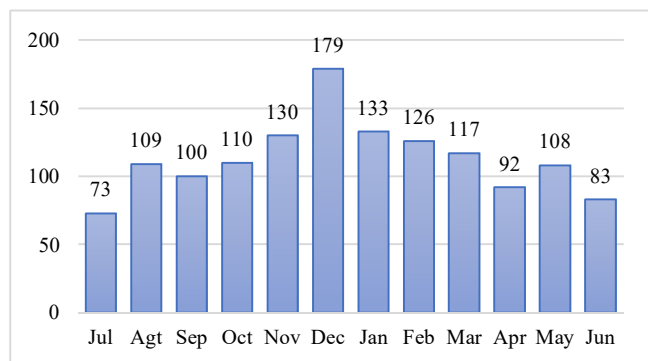


Fig. 2 Total number of SWH from satellite altimetry that crossed Indonesian waters in July 2018 – June 2019

The SWH values at the low-pressure centers around Indonesian waters. Throughout 2018, the maximum SWH value detected from the satellite altimetry was 15 meters on 23 November 2018, at 18:00 UTC. On the other hand, the maximum SWH value from OFS-model occurred in low-pressure areas. There are also moments when satellite altimetry crossed just above the low-pressure center, having different SWH observation values (Table 1). One of the inputs from the OFS-model is the influence of the wind. If there is a cyclone (marked by a low pressure) in an area, the waters traversed by the eye (cyclone) have a much higher SWH value than the surrounding waters [15]. This can be explained by the momentum balance and enthalpy exchange from the ocean's evaporation and then transformed into energy dissipation to form a low pressure in the atmospheric boundary layer [16], [17].

Generally, low-pressure centers are characterized by high SWH in almost evenly manner in each month of 2018. 43% (10 occurrences) of high SWH occurred in the Pacific Ocean waters of the Eastern Philippines. The remaining spreads across the South China Sea, Indian Ocean, Andaman Sea, and Australia's Gulfs. An interesting incident occurred on 02 April 2019, in which a tropical cyclone named Wallace formed around the Northern Waters of Australia ( $10^{\circ}$  south latitude) entered the Banda Sea, Indonesia, on 03 April 2019. It then turned back to the south due to the Coriolis force [18]. This cyclone reached its peak on 07 April 2019, marked by a height of 8 meters SWH, then decayed on 09 April 2019 at a southern latitude of  $150^{\circ}$  with an SWH interval of 3-4 meters. The Wallace cyclone increased the intensity of rainfall in Maluku and surrounding areas, in addition to causing high waves. Data compiled from BMKG shows that on 05 April 2019, moderate-heavy rainfall intensity occurred in Southeast

Sulawesi, Nusa Tenggara Timur (NTT), Maluku, and Papua. In comparison, the wave height of 4.0-6.0 meters occurred in southern Rotte Island, Timor Sea of southern NTT, and the Indian Ocean of southern NTT. A tropical low pressure was also formed in the Southern Java Sea on 24 January 2019, at 21:00 UTC. Yet, its power decayed five days later due to insufficient energy.

The tropical cyclone Wallace was still in the safe category because most of its path occurred in the ocean. Conversely, the Cyclone Pabuk that occurred on 1 January 2019 had been affected differently. This cyclone was initially formed in the central South China Sea at southern latitudes  $5^{\circ}$  [19]. It then strengthened and reached the Gulf of Thailand on 2-4 January 2019, with a maximum SWH of 8 meters. In 5 January 2019, at 06:00 UTC, this cyclone crossed mainland Thailand. At 21:00 UTC, the SWH increased to 7 meters and decays on 06 January 2019 in the Andaman Sea on the same day. The tropical cyclones crossing the mainland need special attention since they impact economic losses and damage [20]. Data collected from [21] revealed that Cyclone Pabuk caused rough seas, damage to public facilities, and thousands of people displaced. Referring to research [22], the Northern Hemisphere (NH) has a higher cyclone frequency but with a much lower trend than the Southern Hemisphere (SH). This is because NH has much land as a form of heat exchange with the ocean; it was the main ingredient for cyclone formation. Reference [23] shows in more detail the heat transfer of the sea to the north through the equator contributing to the warming of the NH seas.

Referring to Table 1, the cyclone with the most tremendous damage and loss in this study was the Mangkhut that occurred in the Philippines' western waters with a total economic loss of \$3.7 billion and at least 130 fatalities [24]. It affected Indonesia with an increase in rainfall in some areas crossed by the cyclone's tail, such as Sumatra, Java, Kalimantan, to Papua. This cyclone caused waves up to 4 meters in height in Indonesia's eastern and southern waters. The occurrence of tropical cyclones in the hemisphere appears with another month. In the NH is generally form in June to November with a peak in August-September (44%). The SH is from November to April with a peak in January-March (66%). However, there was no trend in the increase in the global number of tropical cyclones from 1985-2014, with around 80 tropical cyclones each year worldwide [25].

To add, Table 1 delineates a satellite altimeter trajectory recorded just above the low-pressure center on 24 November 2018 at 18:00-21:00 UTC. The obtained SWH value for satellite altimetry measurement was in accordance with the model, which was 4.5 meters. Whereas on the second occurrence on 19 January 2019, at 18:00 UTC, the SWH value of the satellite altimetry measurement was 1 meter, while in the model, it was 6 meters. The difference suggests the importance of validation using the altimetry data. The technique is often applied in validating a model [26] or validating it with other observation tools [27]. Besides, Indonesian waters have a relatively low SWH ( $<1$ m) compared to their outer waters. This has generally been in accordance with forecasts issued by the Indonesian Marine Meteorological Center, BMKG, except these waters are affected by tropical cyclones.

TABLE I

THE RECAPS OF HIGH SWH DUE TO LOW PRESSURE DETECTED BY THE BMKG-OFS MODEL. THE LIGHT GRAY COLOR SHOWS THE SWH ALTIMETER MEASUREMENTS THAT HIGHER THAN THE MODEL, WHILE THE DARK GRAY COLOR INDICATES THE ALTIMETER MEASUREMENT THAT WAS JUST ABOVE THE LOW-PRESSURE CENTER TO THE MODEL

Start	End	Location	SWH Height (m)	Cyclone name	Peak classification	Pressure (hPa)
04/08/2018 18:00	-		9	-	-	-
10/09/2018 09:00	15/9/2018 18:00	Philippines, Pacific Ocean	20	Mangkhut	Typhoon	905
01/10/2018 06:00	05/10/2018 15:00	Philippines, Pacific	9	Kong-rey	Typhoon	900
24/10/2018 00:00	31/10/2018 21:00	Philippines, Pacific	10	Yutu	Typhoon	900
01/11/2018 00:00	01/11/2018 21:00	Philippines, Pacific	5	Yutu	Typhoon	900
07/11/2018 21:00	08/11/2018 09:00	Flores Sea	10	-	-	-
18/11/2018 06:00	18/11/2018 21:00	Philippines, Pacific	8	Man-yi	Typhoon	960
21/11/2018 18:00	23/11/2018 12:00	South Sea China	14	Man-yi	Typhoon	960
23/11/2018 18:00	-	South Sea China	15	-	-	-
24/11/2018 18:00	24/11/2018 21:00	Philippines, Pacific	4.5	-	-	-
09/12/2018 15:00	-		9	-	-	-
23/12/2018 21:00	31/12/2018 21:00	Philippines, Pacific - South Sea China	9	Usman	Tropical depression	1000
01/01/2019 06:00	06/01/2019 09:00	Gulf of Thailand-Andaman Sea	9	Pabuk	Tropical storm	996
08/01/2019 09:00	-	Pacific Ocean	12	-	-	-
17/01/2019 06:00	20/01/2019 21:00	Philippines, Pacific	7	Amang	Tropical depression	1004
19/01/2019 18:00	-		6	-	-	-
24/01/2019 21:00	29/01/2019 03:00	South Sea Java	7	n/a	Tropical low	1004
28/01/2019 06:00	30/01/2019 09:00	South Sea Java	6	Riley	Severe tropical cyclone	974
21/02/2019 18:00	27/02/2019 06:00	Philippines, Pacific	16	Wutip	Typhoon	920
09/03/2019 18:00	-		8	-	-	-
14/03/2019 03:00	17/03/2019 18:00	Hindia Ocean	8	Savannah	Severe tropical cyclone	951
18/03/2019 03:00	23/03/2019 03:00	Australia Bay	9	Trevor	Severe tropical cyclone	950
02/04/2019 03:00	08/04/2019 03:00	Banda Sea	8	Wallace	Severe tropical cyclone	980

### B. Model Performance

A cumulative stacked bar graph is presented to find out the performance of the SWH-derived model toward the altimetry data (Fig. 3a). The lowest to highest statistical analyses in a row are bias, RMSE, and correlation coefficient for all observations. The lowest bias of 0.26 occurred at 9:00 UTC; the lowest RMSE of 0.48 occurred at 21:00 UTC, and the highest correlation coefficient of 0.82 was obtained at 18:00 UTC. The smaller the bias value, the better the output of the model. The RMSE values indicate the distance or proximity of the distribution of the model results to satellite observations. The lower the value, the better the results of the model used. While the correlation coefficient describes the closeness of the two results: the greater the value, the closer the relationship. Thus, it can be summarized that bias, RMSE, and correlation do not occur at the same time. This is due to the fluctuation of the SWH value as presented in Table 1. The correlation coefficient of 0.69-0.82 was categorized as moderate until a strong positive relationship [28] explained the diversity of satellite data. In Indonesia, water shows similar results that during one month (January) also resulted in a correlation of 0.69 [29]. The verification recapitulation in July 2018 – June 2019 is presented in Fig. 3b. The lowest to highest statistical analysis results in a row are bias, RMSE, and correlation coefficient for the month. This pattern is exactly the same as the observation time of Fig. 3a. The lowest bias and RMSE occurred in November. In the same month, the highest correlation occurred.

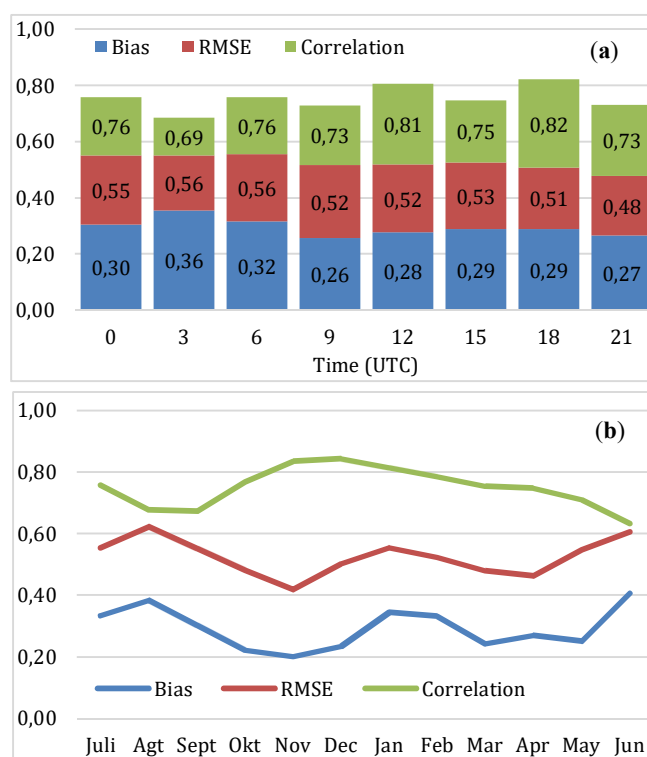


Fig. 3 (a) A cumulative stacked bar graph of the statistical analysis of SWH model verification toward satellite altimetry data every three hours of observation. (b) The plotting line of statistical analysis of SWH model verification of altimetry satellite data in July 2018 – June 2019.

The best combination of statistical analysis was in November. On the contrary, less ideal statistical results occurred in June (Fig. 3b). Compared to the total satellite trajectory (Fig. 2) in the two months, the performance of the model was not affected by the number of trajectories. Thus, the model is said to be quite reliable compared to satellite data. As a comparison, similar results were also conducted on Jason 2 satellite every month [26]. Obtained the mean bias is lower than RMSE, with the mean bias almost equal to zero and RMSE about 0.2-0.4. Furthermore, several recent studies have compared altimetry satellites with various models, such as study [30] comparing the ECMWF IFS (European Centre for Medium-Range Weather Forecasts Integrated Forecasting System) model with Cryosat-2 obtained SWH correlation in NE Atlantic and Pacific by 0.98 and 0.95, respectively. In Indonesia, Sulawesi (Celebes) waters especially, also conducted verification with WW3 model against Jason-2 by determining several types of Jason-2 data, namely WIW19, ALES (Adaptive Leading Edge Subwaveform), and SGDR (Geophysical Data Records Sensor) of 0.72, 0.74, and 0.55, respectively [31]. The low correlation in Sulawesi waters is due to low wind speed, which produces low waves and stronger echo intensity than the surrounding area [32].

The further processing results showed the filtering technique resulted in the least difference in coefficient values obtained. The difference was 1/100 from the initial correlation coefficient ranging from 0.68 to 0.81. Besides, the method's application, by ignoring some of the minimum values of SWH, did not show significant differences in RMSE values and correlation coefficient [33]. This means that satellite altimetry is suitable to be used as a real observation of SWH data. However, it does not cover all areas of water in one measurement.

#### IV. CONCLUSION

This study has successfully verified the OFS-SWH model of satellite altimetry for one the full year (i.e., July 2018 –June 2019). The technique was performed by adjusting the position and time of the altimetry data to the model. The total trajectories fluctuated every month and were obtained with the most trajectories of 179 in December and the lowest of 73 in June. From the whole set of observations, three important pieces of information was obtained: a high SWH is associated with the low-pressure center, a high SWH measurement was detected more through satellite altimetry, and in some cases, satellite altimetry that passes just above the low-pressure center has different SWH value to the model. A total of 17 low-pressure centers (July 2018-June 2019) were formed, in which the Mangkhut tropical cyclone (10 September 2018) had the greatest damage and loss.

The statistical analysis results were analyzed on a three hourly and monthly basis. On the three-hourly basis, the lowest bias 0.26 occurred at 9:00 UTC, the lowest RMSE 0.48 occurred at 21:00 UTC, and the most significant correlation of 0.82 occurs at 18:00 UTC. While on the monthly scale, the lowest bias and RMSE were found in November, and the largest correlation coefficient was in November. In general, these results are not much different from the verification stage carried out every month. In conclusion, this technique can be

an alternative as a new tool to verify maritime weather in the operation of BMKG.

#### ACKNOWLEDGMENT

A profound appreciation is addressed to MMC, *Pusat Meteorologi Maritim* (Pusmetmar), BMKG, Indonesia, and ifremer, France, to offer the data OFS model altimetry respectively so that this research can be completed. We are grateful to the Center for Education and Training, *Pusat Pendidikan dan Pelatihan* (Pusdiklat) BMKG, Indonesia to fund this research with a scholarship scheme.

#### REFERENCES

- [1] I. Alifidini, N. A. P. Iskandar, A. W. Nugraha, D. N. Sugianto, A. Wirasatriya, and A. B. Widodo, "Analysis of ocean waves in 3 sites potential areas for renewable energy development in Indonesia," *Ocean Eng.*, vol. 165, pp. 34–42, 2018, doi: <https://doi.org/10.1016/j.oceaneng.2018.07.013>.
- [2] A. Ribal, A. V. Babanin, S. Zieger, and Q. Liu, "A high-resolution wave energy resource assessment of Indonesia," *Renew. Energy*, vol. 160, pp. 1349–1363, 2020, doi: <https://doi.org/10.1016/j.renene.2020.06.017>.
- [3] A. M. Durán-Rosal, J. C. Fernández, P. A. Gutiérrez, and C. Hervás-Martínez, "Detection and prediction of segments containing extreme significant wave heights," *Ocean Eng.*, vol. 142, pp. 268–279, 2017, doi: <https://doi.org/10.1016/j.oceaneng.2017.07.009>.
- [4] V. G. Grigorjeva, S. K. Gulev, and V. D. Sharmar, "Validating Ocean Wind Wave Global Hindcast with Visual Observations from VOS," *Oceanology*, vol. 60, no. 1, pp. 9–19, 2020, doi: [10.1134/S0001437020010130](https://doi.org/10.1134/S0001437020010130).
- [5] H. Yu *et al.*, "A global high-resolution ocean wave model improved by assimilating the satellite altimeter significant wave height," *Int. J. Appl. Earth Obs. Geoinf.*, vol. 70, pp. 43–50, 2018, doi: <https://doi.org/10.1016/j.jag.2018.03.012>.
- [6] N. Tran, D. Vandemark, E. D. Zaron, P. Thibaut, G. Dibarboure, and N. Picot, "Assessing the effects of sea-state related errors on the precision of high-rate Jason-3 altimeter sea level data," *Adv. Sp. Res.*, 2019, doi: <https://doi.org/10.1016/j.asr.2019.11.034>.
- [7] R. Roscher, B. Uebbing, and J. Kusche, "STAR: Spatio-temporal altimeter waveform retracking using sparse representation and conditional random fields," *Remote Sens. Environ.*, vol. 201, pp. 148–164, 2017, doi: <https://doi.org/10.1016/j.rse.2017.07.024>.
- [8] J. Sommer, E. Chassignet, and A. Wallcraft, "Ocean Circulation Modeling for Operational Oceanography: Current Status and Future Challenges," 2018.
- [9] Y. Quilfen and B. Chapron, "Ocean Surface Wave-Current Signatures From Satellite Altimeter Measurements," *Geophys. Res. Lett.*, vol. 46, no. 1, pp. 253–261, Jan. 2019, doi: <https://doi.org/10.1029/2018GL081029>.
- [10] M. Jiang, K. Xu, and Y. Liu, "Calibration and Validation of Reprocessed HY-2A Altimeter Wave Height Measurements Using Data from Buoy, Jason-2, Cryosat-2, and SARAL/AltiKa," *J. Atmos. Ocean. Technol.*, vol. 35, no. 6, pp. 1331–1352, Jul. 2018, doi: [10.1175/JTECH-D-17-0151.1](https://doi.org/10.1175/JTECH-D-17-0151.1).
- [11] R. Schneider, P. N. Godiksen, H. Villadsen, H. Madsen, and P. Bauer-Gottwein, "Application of CryoSat-2 altimetry data for river analysis and modelling," *Hydrol. Earth Syst. Sci.*, vol. 21, no. 2, pp. 751–764, 2017, doi: [10.5194/hess-21-751-2017](https://doi.org/10.5194/hess-21-751-2017).
- [12] J. Yang, J. Zhang, Y. Jia, F. Chenqing, and W. Cui, "Validation of Sentinel-3A/3B and Jason-3 Altimeter Wind Speeds and Significant Wave Heights Using Buoy and ASCAT Data," *Remote Sens.*, vol. 12, p. 2079, Jun. 2020, doi: [10.3390/rs12132079](https://doi.org/10.3390/rs12132079).
- [13] C. M. Appendini, V. Camacho-Magaña, and J. A. Breña-Naranjo, "ALTWAVE: Toolbox for use of satellite L2P altimeter data for wave model validation," *Adv. Sp. Res.*, vol. 57, no. 6, pp. 1426–1439, 2016, doi: <https://doi.org/10.1016/j.asr.2015.12.015>.
- [14] C. M. Appendini, A. Torres-Freyermuth, P. Salles, J. López-González, and E. T. Mendoza, "Wave Climate and Trends for the Gulf of Mexico: A 30-Yr Wave Hindcast," *J. Clim.*, vol. 27, no. 4, pp. 1619–1632, Feb. 2014, doi: [10.1175/JCLI-D-13-00206.1](https://doi.org/10.1175/JCLI-D-13-00206.1).
- [15] S. Yang and J. Oh, "Long-Term Changes in the Extreme Significant Wave Heights on the Western North Pacific: Impacts of Tropical

- Cyclone Activity and ENSO,” *Asia-Pacific J. Atmos. Sci.*, vol. 54, no. 1, pp. 103–109, 2018, doi: 10.1007/s13143-017-0063-y.
- [16] F. Zhang and K. Emanuel, “On the Role of Surface Fluxes and WISHE in Tropical Cyclone Intensification,” *J. Atmos. Sci.*, vol. 73, p. 160309141253007, Mar. 2016, doi: 10.1175/JAS-D-16-0011.1.
- [17] L. Zhang and L. Oey, “An Observational Analysis of Ocean Surface Waves in Tropical Cyclones in the Western North Pacific Ocean,” *J. Geophys. Res. Ocean.*, vol. 124, no. 1, pp. 184–195, Jan. 2019, doi: 10.1029/2018JC014517.
- [18] J. Nakamura *et al.*, “Western North Pacific Tropical Cyclone Model Tracks in Present and Future Climates,” *J. Geophys. Res. Atmos.*, vol. 122, no. 18, pp. 9721–9744, Sep. 2017, doi: <https://doi.org/10.1002/2017JD027007>.
- [19] C. D. M. Safuan, N. H. Roseli, Z. Bachok, M. F. Akhir, C. Xia, and F. Qiao, “First record of tropical storm (Pabuk - January 2019) damage on shallow water reef in Pulau Bidong, south of South China Sea,” *Reg. Stud. Mar. Sci.*, vol. 35, p. 101216, 2020, doi: <https://doi.org/10.1016/j.rsma.2020.101216>.
- [20] M. Lenzen, A. Malik, S. Kenway, P. Daniels, K. L. Lam, and A. Geschke, “Economic damage and spill-overs from a tropical cyclone,” *Nat. Hazards Earth Syst. Sci. Discuss.*, pp. 1–28, Jan. 2018, doi: 10.5194/nhess-2017-440.
- [21] P. Pavarangoon *et al.*, “Development of international mirroring system for real-time web of meteorological satellite data,” *Earth Sci. Informatics*, vol. 13, no. 4, pp. 1461–1476, 2020, doi: 10.1007/s12145-020-00488-z.
- [22] J. Song, P. J. Klotzbach, J. Tang, and Y. Wang, “The increasing variability of tropical cyclone lifetime maximum intensity,” *Sci. Rep.*, vol. 8, no. 1, p. 16641, 2018, doi: 10.1038/s41598-018-35131-x.
- [23] S. M. Kang, R. Seager, D. M. W. Frierson, and X. Liu, “Croll revisited: Why is the northern hemisphere warmer than the southern hemisphere?,” *Clim. Dyn.*, vol. 44, no. 5, pp. 1457–1472, 2015, doi: 10.1007/s00382-014-2147-z.
- [24] H.-S. Lo *et al.*, “Impacts of Typhoon Mangkhut in 2018 on the deposition of marine debris and microplastics on beaches in Hong Kong,” *Sci. Total Environ.*, vol. 716, p. 137172, Feb. 2020, doi: 10.1016/j.scitotenv.2020.137172.
- [25] H. Ramsay, “The Global Climatology of Tropical Cyclones.” Oxford University Press, 2017, doi: 10.1093/acrefore/9780199389407.013.79.
- [26] X. Ye, M. Lin, and Y. Xu, “Validation of Chinese HY-2 satellite radar altimeter significant wave height,” *Acta Oceanol. Sin.*, vol. 34, no. 5, pp. 60–67, 2015, doi: 10.1007/s13131-015-0667-y.
- [27] A. Carret, F. Birol, C. Estournel, B. Zakardjian, and P. Testor, “Synergy between in situ and altimetry data to observe and study Northern Current variations (NW Mediterranean Sea),” *Ocean Sci.*, vol. 15, pp. 269–290, Mar. 2019, doi: 10.5194/os-15-269-2019.
- [28] N. Gogtay and U. Thatte, “Principles of Correlation Analysis,” *J. Assoc. Physicians India*, vol. 65, pp. 78–81, Mar. 2017.
- [29] E. Supriyadi, “Verification of Significant Wave Height Ocean Forecast System (OFS)-BMKG using Altimetry Satellite,” *J. Meteorol. dan Geofis.*, vol. 19, no. 2, pp. 93–102, 2019, doi: <http://dx.doi.org/10.31172/jmg.v19i2.586>.
- [30] S. Abdalla, S. Dinardo, J. Benveniste, and P. A. E. M. Janssen, “Assessment of CryoSat-2 SAR mode wind and wave data,” *Adv. Sp. Res.*, vol. 62, no. 6, pp. 1421–1433, 2018, doi: <https://doi.org/10.1016/j.asr.2018.01.044>.
- [31] K. Ichikawa, X.-F. Wang, and H. Tamura, “Capability of Jason-2 Subwaveform Retracker for Significant Wave Height in the Calm Semi-Enclosed Celebes Sea,” *Remote Sens.*, vol. 12, p. 3367, Oct. 2020, doi: 10.3390/rs12203367.
- [32] X. Wang, K. Ichikawa, and D. Wei, “Coastal Waveform Retracking in the Slick-Rich Sulawesi Sea of Indonesia, Based on Variable Footprint Size with Homogeneous Sea Surface Roughness,” *Remote Sens.*, vol. 11, p. 1274, May 2019, doi: 10.3390/rs11111274.
- [33] S. A. Myslenkov and A. Chernyshova, “Comparing wave heights simulated in the Black Sea by the SWAN model with satellite data and direct wave measurements,” *Russ. J. Earth Sci.*, vol. 16, pp. 1–12, Nov. 2016, doi: 10.2205/2016ES000579.